

The transcription factor Spt4-Spt5 complex regulates the expression of ATG8 and ATG41

Xin Wen^a, Damián Gatica^a, Zhangyuan Yin^a, Zehan Hu^b, Jörn Dengjel^b, and Daniel J. Klionsky ^a

^aLife Sciences Institute, and the Department of Molecular, Cellular and Developmental Biology, University of Michigan, Ann Arbor, MI, USA;

^bDepartment of Biology, University of Fribourg, Fribourg, Switzerland

ABSTRACT

Macroautophagy/autophagy, a highly conserved dynamic process, is one of the major degradative pathways in cells. So far, over 40 autophagy-related (ATG) genes have been identified in *Saccharomyces cerevisiae*, most of which have homologs in more complex eukaryotes. Autophagy plays a crucial role in cell survival and maintenance, and its dysfunction is related to various diseases, indicating that the proper regulation of autophagy is important. Although the overall process of autophagy has been extensively studied, in particular with regard to the function of the Atg proteins, relatively little is known about the regulatory mechanisms that control autophagy activity. Spt5 is one of the transcriptional factors that is universally conserved across all domains. This protein can form a complex with Spt4, together playing a central role in transcription. In complex eukaryotic cells, the Spt4-Spt5 complex plays a dual role in gene regulation, acting both to delay transcription through promoter-proximal pausing, and to facilitate transcriptional elongation. In contrast, in *S. cerevisiae*, only the positive function of the Spt4-Spt5 complex has been identified. Here, we show for the first time that the Spt4-Spt5 transcription factor complex negatively regulates ATG genes in *S. cerevisiae*, inhibiting autophagy activity during active growth. Under autophagy-inducing conditions, the repression is released by Spt5 phosphorylation, allowing an upregulation of autophagy activity.

KEYWORDS

Autophagy; Spt4; Spt5; stress; vacuole; yeast

Abbreviations: AID: auxin-inducible degen; ATG: autophagy-related; ChIP: chromatin immunoprecipitation; Cvt: cytoplasm-to-vacuole targeting; DSIF: DRB sensitivity-inducible factor; NELF: negative elongation factor; ORF: open reading frame; PA: protein A; PE: phosphatidylethanolamine; prApe1: precursor aminopeptidase I; RT-qPCR: real-time quantitative PCR; RNAP II: RNAPolymerase II; TSS: transcription start site; WT: wild-type

Introduction

Autophagy, a term from the Greek words “auto” (self) and “phagein” (to eat), is a highly regulated degradative process that allows cells to break down their own components within the vacuole in yeast and plants, or the lysosome in more complex eukaryotes [1,2]. A basal level of autophagy is usually maintained in physiological conditions, while in response to different stimuli (e.g., nutrient limitation, hypoxia and other stress conditions), autophagy is induced. Depending on how substrates are transported, autophagy is divided into 2 main types (macroautophagy and microautophagy) in yeast, whereas additional types of autophagic pathways including chaperone-mediated autophagy, chaperone-assisted selective autophagy and endosomal microautophagy exist in mammals [3]. Both macroautophagy and microautophagy have nonselective and selective modes: the nonselective process refers to the turnover of bulk cytoplasm, whereas the selective pathway can specifically target damaged or superfluous organelles, protein aggregates, invasive pathogens and other intracellular components [4]. In this paper, we mainly focus on yeast

nonselective macroautophagy (hereafter autophagy), in which random cytoplasm is first sequestered within the phagophore, a transient double-membrane structure. The phagophore then expands and matures into a large cytoplasmic double-membrane vesicle termed the autophagosome [5]. Once completed, the outer membrane of the autophagosome fuses with the vacuole, allowing the inner membrane and cargo to become exposed to the luminal contents of this organelle and degraded by resident hydrolases [6]. The breakdown products are finally released back into the cytosol to recycle the macromolecular constituents, and to generate energy to maintain cell viability under unfavorable conditions [7].

Our understanding of the molecular mechanism of autophagy has greatly been advanced by yeast genetic studies in the past 2 decades. So far, more than 40 autophagy-related (ATG) genes have been identified in yeast, and most of the corresponding protein products are important factors that function to initiate, complete and regulate autophagy [8,9]. Because most work has focused on the basic mechanism, how auto-phagy is regulated still remains largely unexplored. In

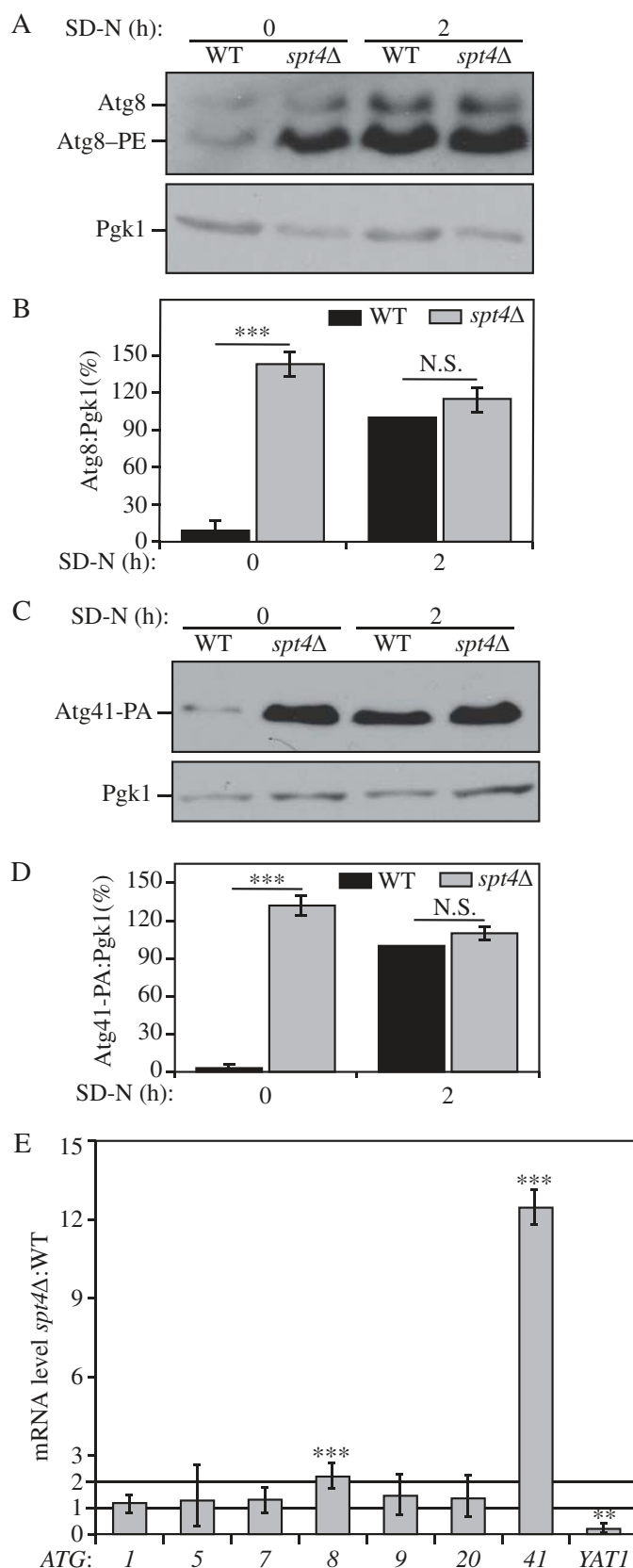


Figure 1. Spt4 negatively regulates *ATG8/Atg8* and *ATG41/Atg41* expression in growing conditions. **(A-D)** Analysis of Atg8 and Atg41 protein levels. Protein extracts were generated from **(A)** wild-type (TVY1, *pep4Δ*) and *spt4Δ* (WXY100, *pep4Δ*) cells, or **(C)** wild-type (ZYY108) and *spt4Δ* (WXY114) cells expressing Atg41-PA, after growth in YPD to mid-log phase (growing conditions) and shifted to SD-N medium for 2 h (nitrogen starvation). Western blots were probed with anti-Atg8, anti-PA and anti-Pgk1 (loading control) antisera or antibodies. **(B and D)** Quantitative analysis of Atg8 and Atg41 protein levels, respectively. The protein level of either Atg8 or Atg41-PA after 2 h of starvation was set as 1 and other values were normalized; the error bar represents the SEM of at least 3 independent experiments. N.S., not significant, ***, $p < 0.005$. **(E)** Wild-type (WLY176) and *spt4Δ* (WXY105) cells were cultured until mid-log phase and collected in growing conditions. mRNA levels were quantified by RT-qPCR. The mRNA level of different *ATG* genes and *YAT1* (negative control) in *spt4Δ* cells were normalized to that of the corresponding genes in wild-type cells, which was set as 1. Error bars represent the SEM of at least 3 independent experiments; two-tailed t test was used for statistical significance. p values are reported for the comparison between WT and *spt4Δ* strains in growing conditions. **, $p < 0.01$; ***, $p < 0.005$.

particular, little is known about the complicated modulation of gene expression and specific transcriptional regulators of autophagy. The dysfunction of autophagy resulting from altered *ATG* gene expression is related to various human diseases, indicating the importance of proper regulation of autophagy at the transcription level [10]. In *S. cerevisiae*, a dramatic increase in *ATG8* and *ATG41* mRNA transcripts occurs when autophagy is induced, leading to a significant rise in the corresponding protein levels. Moreover, the expression level of Atg8 correlates with autophagosome size, whereas that of Atg41 is related to the frequency of autophagosome formation [11,12]. These results suggest that transcriptional control—and especially that of *ATG8* and *ATG41*—is important in modulating autophagy [11,13]. Our lab showed that the transcriptional regulator Ume6 can negatively modulate autophagy, by binding to the promoter region of *ATG8* in growing conditions [13]. Another recently published study showed that the positive transcriptional regulator Gcn4 regulates *ATG41* during starvation-induced autophagy [11]. Here, we decided to further investigate autophagy regulation through transcriptional modulation.

Transcription, accomplished by RNA polymerase II (RNAP II), is a dynamic and highly regulated process. The success of transcription requires contributions from different transcription accessory factors, one of which is the heterodimeric Spt4-Spt5 complex [14]. This complex can tightly associate with RNAP II in a transcription-dependent manner, and many studies have identified its essential role in promoting transcription elongation [14]. The homolog of the Spt4-Spt5 complex in complex eukaryotes, DRB sensitivity-inducible factor (DSIF, composed of SUPT4H1 and SUPT5H), also shows inhibitory activities in the early stage of transcription [15]. DSIF works with another multi-subunit complex, the negative elongation factor (NELF) to impart a promoter-proximal pausing mechanism to regulate RNAP II activity [16]. This repressive state can be overcome by the positive transcription elongation factor b (P-TEFb) complex, phosphorylating POLR2A/RPB1 (the largest subunit of RNAP II) and the DSIF-NELF complex, which not only causes dissociation of NELF from RNAP II but also changes the DSIF status to promote transcription elongation [17–19]. Because there is no clear evidence showing the presence of NELF in yeast, most studies have only focused on the positive role of the Spt4-Spt5 complex in this organism. A recently published study does point out that there is a pause in early elongation specific to *S. pombe*, which resembles promoter-proximal pausing in metazoans [20], but it still remains an open question as to whether the Spt4-Spt5 complex can play a dual role in transcription in *S. cerevisiae*.

Here, we show that Spt4 may work as a negative transcriptional regulator of autophagy in *S. cerevisiae*. The deletion of *SPT4* leads to an increase in both mRNA and protein levels of *ATG8*/Atg8 and *ATG41*/Atg41 in growing conditions, and these changes correlate with an upregulated level of autophagy. During starvation, we observe a higher level of Spt5 phosphorylation, and the Sgv1/Bur1-Bur2 kinase complex, a homolog of P-TEFb, is responsible for this modification. The dephosphorylation of Spt5 or a transient loss of this protein results in autophagy deficiency and a clear reduction in *ATG41*/Atg41 expression, suggesting that Spt4 and Spt5 may play a distinct role in regulating autophagy. Chromatin immunoprecipitation (ChIP) analysis indicates

that the Spt4-Spt5 complex can interact with DNA regions downstream of the transcription start site (TSS) on *ATG41* in an Spt4-dependent manner in growing conditions. Taking all of the data together, we show for the first time a negative function of Spt4 in budding yeast, and provide the first identification of a negative regulator of *ATG41* expression. In addition, these studies also advance our understanding of the fine-tuned regulation of autophagy at the transcriptional level.

Results

Spt4 negatively regulates the transcription of *ATG8* and *ATG41* in growing conditions

The Spt4-Spt5 complex functions as a transcriptional factor, acting to promote transcription elongation in yeast. However, many regulatory factors have opposite effects on *ATG* genes relative to genes encoding proteins that function primarily during vegetative growth. Accordingly, we decided to examine the effect of mutations in Spt4 and Spt5 on *ATG* gene expression. *SPT5* is an essential gene; we therefore started our analysis with an *spt4Δ* strain. Initially, we focused on *ATG8* and *ATG41*, because these genes show the greatest increase in synthesis following autophagy induction. Furthermore, the Atg8 and Atg41 protein levels provide rapid indirect indicators for transcriptional induction of autophagy.

Protein extracts were prepared from cells in growing conditions and analyzed by western blot. When testing the protein level of Atg8, in both wild-type (WT) and mutant strains, we deleted the *PEP4* gene. Pep4 is a key hydrolase needed to activate many vacuolar enzymes; *pep4Δ* cells are largely protease defective [21]. It is important to use this background to monitor Atg8 protein levels. This is due to the fact that Atg8 (in the form conjugated to phosphatidylethanolamine [PE]) lines both sides of the phagophore and remains attached to the inner surface of the completed autophagosome; this portion of Atg8 is delivered to the vacuole and degraded, but this degradation is blocked in the absence of Pep4 [12]. Thus, the WT strain we refer to in this experiment actually corresponds to *pep4Δ*.

We observed a consistent increase in the Atg8 protein level (which was detected primarily as Atg8-PE) in growing conditions (SD-N, $t = 0$ h) in an *spt4Δ* strain relative to the WT control (Figure 1A,B). To determine the protein level of Atg41, we integrated a protein A (PA) epitope tag at the C terminus of *ATG41* at the chromosomal locus. Moreover, we used a *PEP4* WT strain to examine the Atg41 protein level because Atg41 is not degraded within the vacuole. As with Atg8, we observed a massive upregulation of Atg41 in growing conditions when *SPT4* was deleted (Figure 1C,D). In contrast, upon starvation (SD-N, $t = 2$ h), the difference in Atg8 and Atg41 protein levels between WT and *spt4Δ* cells was not significant (Figure 1B,D), suggesting that the predominant negative effect of Spt4 on autophagy may take place in growing conditions; the protein level of Spt4 was similar under both growing and starvation conditions (Figure S1A), indicating that the increase in Atg8-PE and Atg41 in the WT strain relative to the *spt4Δ* mutant during starvation was not due to the loss of Spt4 in the former.

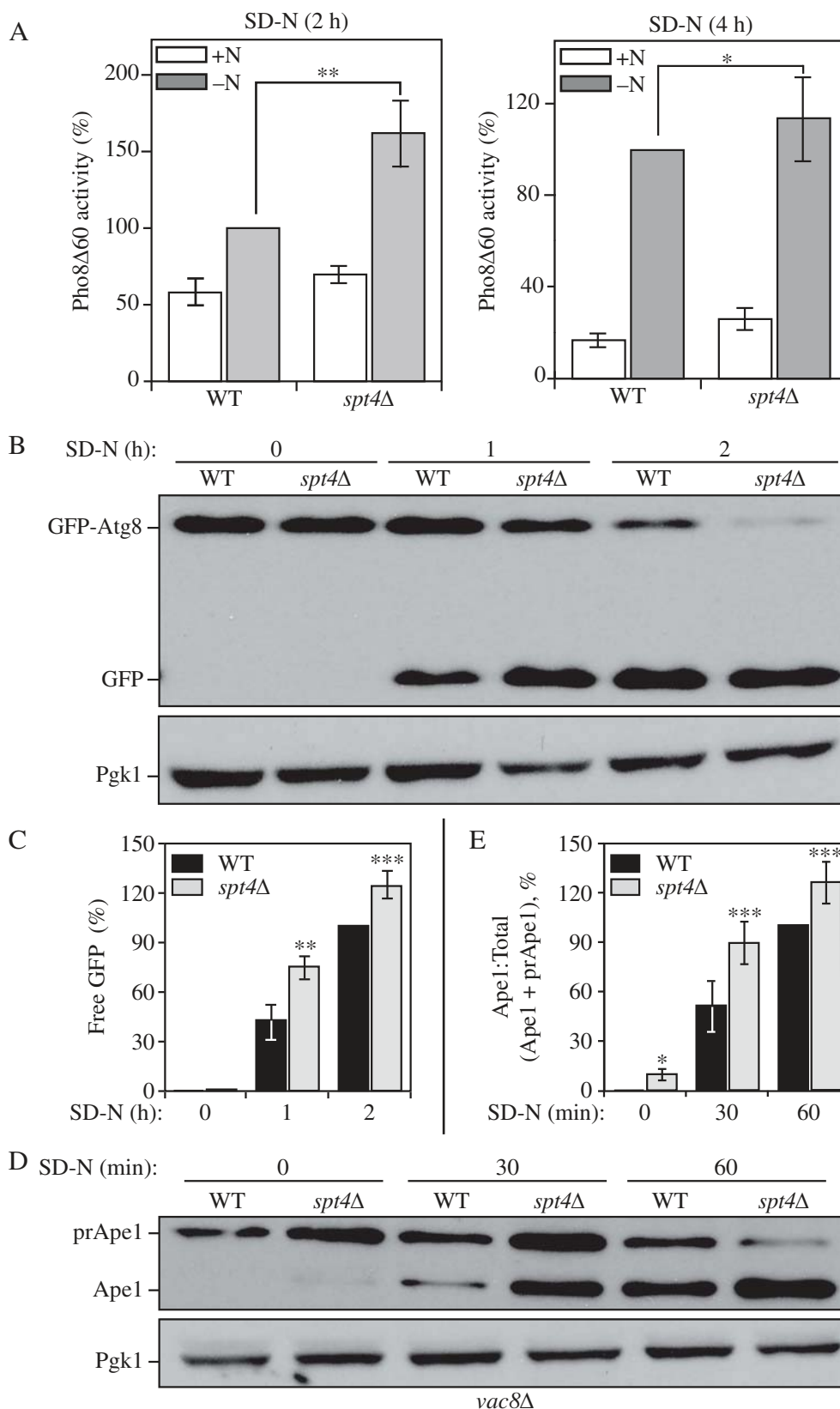


Figure 2. Spt4 negatively regulates autophagy activity. **(A)** Autophagy activity was measured with the quantitative Pho8Δ60 assay in WT (JMY347) and *spt4Δ* (WXY131) cells under growing conditions (+N) and after 2 or 4 h of nitrogen starvation (-N). Error bars represent the SEM of at least 3 independent experiments. *, $p < 0.05$; **, $p < 0.01$. **(B-C)** Autophagy activity was measured using the GFP-Atg8 processing assay. Wild-type (WXY112) and *spt4Δ* cells (WXY113) with *CUP1* promoter-driven *GFP-ATG8* were grown to mid-log phase in YPD and then starved (SD-N) for the indicated times. Samples from growing (YPD, 0 h) and starvation (SD-N, $t = 1-2$ h) conditions were collected. Proteins were analyzed by western blot with anti-YFP antibody and anti-Pgc1 (loading control) antiserum. The quantitative analysis of processed GFP is shown in (C), and the error bar represents the SEM of 3 independent experiments. The processed GFP after 2 h of starvation was set as 1, and other values were normalized. *, $p < 0.05$; **, $p < 0.01$. **(D-E)** Wild-type (WXY121) and *spt4Δ* (WXY122) cells with a deletion of *VAC8* were collected in both growing (YPD) and starvation (SD-N, $t = 30-60$ min) conditions. The precursor (pr) and mature forms of Ape1 were separated by SDS-PAGE and detected with anti-Ape1 antiserum by western blot. Pgc1 was used as a loading control. The ratio of processed Ape1 was quantified in (E), and the error bar represents the SEM of 3 independent experiments. The maturation of prApe1 after 60 min of starvation has been set as 1, and other values were normalized. *, $p < 0.05$; ***, $p < 0.005$.

Next, we examined the mRNA levels of *ATG8*, *ATG41* and other *ATG* genes in both WT and *spt4Δ* cells, by real-time quantitative PCR (RT-qPCR; Figure 1E). There was a relative increase of *ATG8* and an especially significant *ATG41* increase during the vegetative stage in *spt4Δ* cells, whereas no obvious change was observed for the other *ATG* genes that we examined. We used *YAT1* as a control in this analysis (Figure 1E). *YAT1* expression is downregulated in *spt4Δ* cells, presumably due to the loss of Spt4-dependent transcription elongation [22]. As expected, we found a decrease in *YAT1* expression in the absence of Spt4. We also examined the protein levels of some Atg proteins for which there was no obvious difference in gene expression in the *spt4Δ* cells, and observed no significant change in protein amount relative to the WT (Figure S1B–D). Therefore, in growing conditions, Spt4 acts as a negative regulator in modulating the expression of at least *ATG8* and *ATG41* at the transcriptional level, a phenotype that is opposite to the known positive transcriptional role of Spt4.

Cells lacking Spt4 display increased autophagy activity

To test whether Spt4 can regulate autophagy activity, we applied 3 different well-established assays to measure autophagy activity in WT and *spt4Δ* cells. First, we measured autophagy activity using the quantitative Pho8Δ60 assay. In *S. cerevisiae*, *PHO8* encodes a vacuolar phosphatase that is delivered to the vacuole through the secretory pathway, leading to the activation of phosphatase activity [23]. We generated a truncated form of Pho8, Pho8Δ60, which lacks the N-terminal transmembrane domain and can only transit to the vacuole through nonselective autophagy [24]. Thus, by measuring the phosphatase activity in cells expressing only Pho8Δ60, we can measure autophagy flux. A significant increase in autophagy activity was observed in *spt4Δ* cells in 2-h nitrogen-starvation conditions compared to the WT cells (Figure 2A). This upregulated autophagy activity could also be seen in the mutant cells after a longer period of starvation, although the difference relative to the WT was reduced; this change likely reflects the fact that the negative effect of Spt4 is blocked in WT cells under starvation conditions so that the greatest difference is seen shortly after shifting out of growing conditions.

We then used the GFP-Atg8 processing assay. The principle behind this assay relies on the delivery of the population of GFP-Atg8 that is attached on the inner membrane of the autophagosome and exposed to the vacuolar hydrolases following autophagosome-vacuole fusion. Compared to Atg8, GFP is more resistant to degradation; thereby, free GFP is generated in the vacuole lumen, and the conversion of GFP-Atg8 into GFP can be a readout for nonselective autophagic degradation [25]. Because we determined that Spt4 can influence *ATG8*/Atg8 expression, we used the exogenous *CUP1* promoter to drive GFP-Atg8 expression, thus eliminating Spt4-dependent effects. We observed an increasing amount of GFP-Atg8 processing in both WT and *spt4Δ* cells after starvation (SD-N), with more free GFP detected in *spt4Δ* cells compared to the WT (Figure 2B,C), indicating an elevated level of autophagy activity in the mutant cells.

To further support the results from the previous 2 assays, we used another method to monitor autophagy, which relies on the processing of precursor aminopeptidase I (prApe1). Ape1 is a resident vacuolar hydrolase that is initially synthesized as a cytosolic precursor with an N-terminal propeptide. The prApe1 can be delivered to the vacuole through either macroautophagy or the cytoplasm-to-vacuole targeting (Cvt) pathway. Furthermore, this analysis can be conducted similar to a pulse-chase assay by taking advantage of the *vac8Δ* phenotype. In the absence of *VAC8*, prApe1 processing is blocked under vegetative conditions; upon starvation (that is, following autophagy induction), prApe1 is delivered to the vacuole through a process that still requires a receptor and scaffold protein for maximal efficiency [26]. Following delivery, prApe1 is processed to a mature, lower molecular mass species; thereby, we can monitor vacuolar delivery by western blot. As expected, in WT (*vac8Δ*) cells there was essentially no mature Ape1 in growing conditions (SD-N, $t = 0$), and a clear increase in this species with increasing time in starvation conditions (Figure 2D,E). We detected a higher level of prApe1 processing in *spt4Δ vac8Δ* cells with a faint band corresponding to mature Ape1 visible even at the 0 h time point, again suggesting an increase in autophagy activity.

Taken together, these results indicate that there is an elevated level of autophagy in *spt4Δ* cells, suggesting that Spt4 negatively regulates this process, and that the deletion of *SPT4* releases this repressive effect.

Spt5 phosphorylation correlates with the upregulation of ATG41 expression and increased autophagy activity during starvation

After starvation, the protein levels of Atg8 and Atg41 in the WT strain are almost equivalent to those in the *spt4Δ* mutant (Figure 1B,D); this is not due to changes in the Spt4 protein level (Figure S1A). In addition, there was no further increase in the protein amounts in *spt4Δ* cells, indicating that there is probably a mechanism for the release of Spt4-dependent negative regulation when autophagy is induced. Spt4 is a small protein with limited known functions, but its partner, Spt5, is required for transcription; previous reports have shown that the phosphorylation of SUPT5H/Spt5 is especially critical for processive transcription elongation [17]. Therefore, we decided to examine the phosphorylation status of yeast Spt5 under starvation conditions and determine whether this modification can reverse the negative effect of Spt4.

We first used an Spt5-PA strain to monitor the expression and mobility of Spt5 in both nutrient-rich and nutrient-deprived conditions. In +N conditions we detected a single band of the expected molecular mass (150 kDa) for Spt5-PA (Figure 3A). When we starved cells, we again saw a band of 150 kDa, and a second band displaying reduced mobility. The same experiment was repeated using strains in which Spt5 was tagged with GFP and MYC, and we observed the same result—a single band in +N conditions, and a second band of higher molecular mass under starvation conditions (Figure 3A). Liu et al. (2009) generated antisera specific for the phosphorylated form of a 6-amino-acid consensus sequence

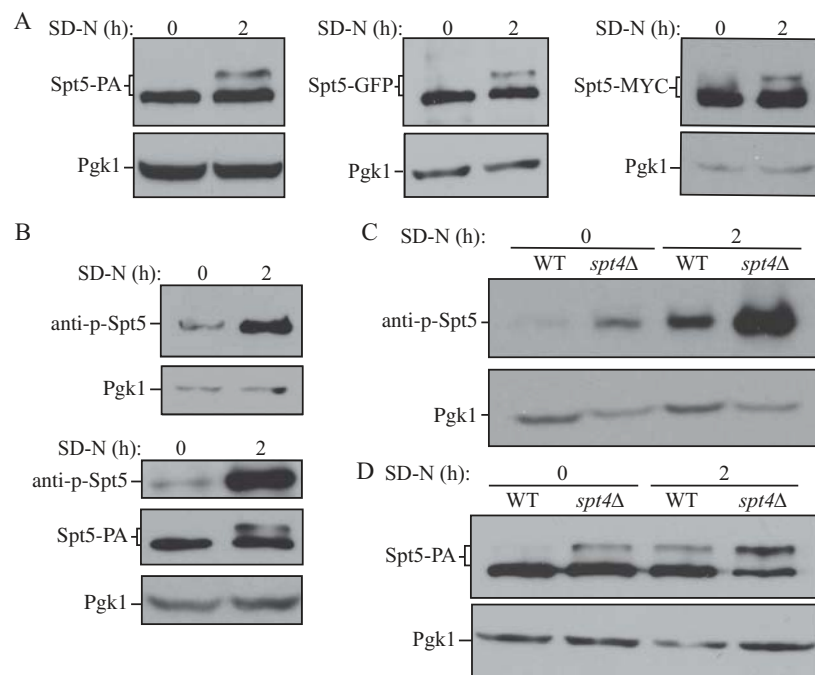


Figure 3. Spt5 phosphorylation is enhanced after starvation or in the absence of Spt4. **(A)** The protein A (PA)-, GFP- and MYC-tagged Spt5 strains (WXY102, WXY107, DGY047) were collected in growing (YPD, mid-log phase) and starvation (SD-N, t = 2 h) conditions. The samples were separated by SDS-PAGE and detected by western blot with anti-PA, anti-YFP or anti-MYC antibodies. Anti-Pgk1 antiserum was used to detect the loading control. **(B)** Wild-type (SEY6210) cells were grown to mid-log phase in growing conditions (YPD) and then starved (SD-N) for 2 h. Samples under these 2 conditions were collected and analyzed by western blot. An antibody specific for the phosphorylated form of Spt5 (anti-p-Spt5) was used to detect the phosphorylated band (upper blot). We also examined phosphorylation in a strain expressing Spt5 tagged with PA (WXY102); the total protein level of Spt5 was detected with anti-PA and the phosphorylation of Spt5 was monitored with the anti-p-Spt5 antibody (lower blot) **(C)** Samples from wild-type (WLY176) and *spt4Δ* (WXY105) strains were collected in both growing (YPD) and starvation (SD-N, t = 2 h) conditions for western blot analysis. Spt5 phosphorylation was monitored with the anti-p-Spt5 antibody. **(D)** The Spt5-PA level of wild-type (WXY102) and *spt4Δ* (WXY103) cells in growing (YPD) and starvation (SD-N) conditions was detected by western blot with anti-PA antibodies.

derived from 15 repeats in the C terminus of Spt5 (anti-p-Spt5) [27]. Using this anti-p-Spt5 antibody, we detected a faint band in growing conditions, which became more intense after starvation, whereas the total protein amount of Spt5 remained at a similar level in both growing and starvation conditions (Figure 3B). To further examine the effect of Spt4 on regulation, we examined potential Spt5 phosphorylation in the *spt4Δ* strain. The phosphorylation of Spt5 was more obvious in *spt4Δ* cells than WT cells under growing conditions, and it was massively increased after starvation (Figure 3C). Using Spt5-PA and *spt4Δ* Spt5-PA strains, we detected a band shift of Spt5 in *spt4Δ* cells in growing conditions, similar to the level seen in WT cells following autophagy induction (Figure 3D). The above results suggest that Spt5 can be further phosphorylated under autophagy-inducing conditions, and there is an increased level of Spt5 phosphorylation in the absence of Spt4.

We next examined whether interfering with Spt5 phosphorylation would influence ATG expression and autophagy activity. Based on information from several previous studies [27–29], we decided to carry out site-directed mutagenesis on the last 7 serine residues (S1009, S1015, S1025, S1032, S1043, S1052, S1058) in the C terminus of Spt5. Conversion of these residues to alanine resulted in the generation of a nonphosphorylatable mutant, Spt5[S7A]. A clear mobility difference was observed between WT and Spt5[S7A] cells after starvation, indicating the relative absence of

phosphorylation of Spt5 in Spt5[S7A]-expressing cells (Figure 4A). We further applied the GFP-Atg8 assay to test autophagy activity, which showed a significantly decreased GFP-Atg8 processing in mutant cells after starvation (Figure 4B,C); therefore auto-phagy activity was reduced when Spt5 phosphorylation was blocked. As predicted based on these results, Spt5[S7A] cells exhibited decreased mRNA and protein levels of *ATG41/Atg41* in the nutrient-deficient condition, whereas there was no difference under growing conditions (Figure 4D,E). However, the influence of Spt5 dephosphorylation on *ATG8* mRNA level was not obvious, indicating that Spt5 may play a role primarily in regulating *ATG41* (Figure S2A).

We also established a phosphomimetic form of the protein Spt5[S7E] by mutating the Spt5 serine residues in the C terminus to glutamate. We first measured autophagic activity in both Spt5[S7A] and Spt5[S7E] cells using the quantitative Pho8Δ60 assay. Compared to WT cells, Spt5[S7A] showed a decrease of autophagy activity, whereas the Spt5 [S7E] mutant exhibited upregulated autophagy activity after 4 h of starvation (Figure S2B). The GFP-Atg8 processing assay also indicated that autophagy activity was enhanced in Spt5 [S7E] cells (Figure S2C,D). Because Spt5 phosphorylation is maintained at a basal level in growing conditions and is further upregulated after starvation, the most obvious phenotype of the phosphomimetic mutant should be observed in nutrient-rich conditions. In agreement with our hypothesis,

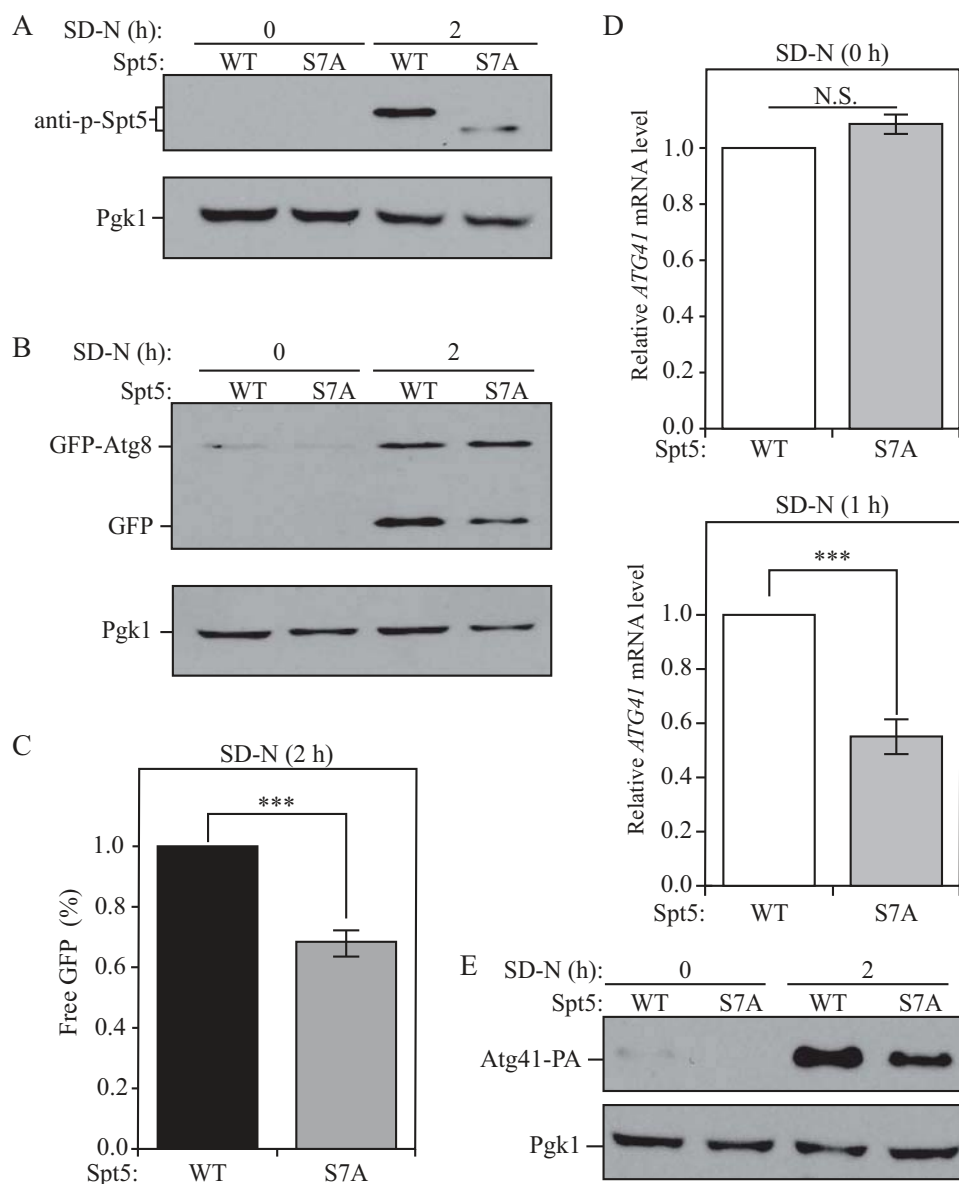


Figure 4. Dephosphorylation of Spt5 negatively modulates autophagy by downregulating *ATG41* mRNA and protein levels after starvation. **(A)** Samples collected from cells expressing WT (DGY047) and nonphosphorylatable Spt5 (DGY048) were analyzed by western blot. The phosphorylation of Spt5 was detected with the specific anti-p-Spt5 antibody. **(B-C)** Autophagy activity was measured by GFP-Atg8 processing in WT (DGY050) and Spt5[S7A] (DGY051) cells harboring endogenous *GFP-ATG8* plasmids under growing conditions and after 2 h of starvation. The quantitative analysis of processed GFP after starvation (there is no processed GFP in the growing condition) is shown in (C), and the error bar represents the SEM of 3 independent experiments. The processed GFP of the WT strain after starvation was set as 1, and other values were normalized. ***, $p < 0.005$. **(D)** The mRNA level of *ATG41* in WT (DGY047) and Spt5[S7A] (DGY048) cells was measured by RT-qPCR under growing conditions and starvation (SD-N, 1 h). The error bar represents the SEM of 3 independent experiments, and p values are reported for the comparison between the wild-type and Spt5[S7A] strains during starvation. N.S., not significant, ***, $p < 0.005$. **(E)** The anti-PA antibody was used to detect Atg41-PA in samples (WT, WXY127; Spt5[S7A], WXY128) collected from growing and starvation (SD-N, 2 h) conditions by western blot analysis.

the mRNA level of *ATG41* showed a slight increase in the Spt5[S7E]-expressing cells in growing conditions, while the Atg41 protein level did not change compared to the WT in both growing and starvation conditions, suggesting that the slight increase in *ATG41* mRNA level was not sufficient to drive a detectable upregulation of the protein level (Figure S2E,F). Thus, with the Spt5[S7E] mutant, a positive role in transcription elongation of other factors may account for the observed increase in autophagy activity.

Because *SPT5* is an essential gene, we took advantage of an auxin-inducible degron (AID) system to generate an Spt5-inducible degradation strain [30]. After 30 min of auxin

treatment, Spt5 protein levels were undetectable in the Spt5-inducible degradation strain (Spt5-AID-MYC), which provided us with a method to conditionally control the expression of this protein (Figure S3A). With this strain, we used the GFP-Atg8 processing assay to test autophagy activity. We found that the autophagy activity decreased when Spt5 was temporally depleted (Figure S3B,C). Correspondingly, the expression of *ATG41*/Atg41 decreased when applying auxin treatment to the Spt5-AID strain (Figure S3D,E). Therefore, in contrast to Spt4, Spt5 appears to always play a positive role in regulating autophagy, which agrees with its essential role in transcription elongation.

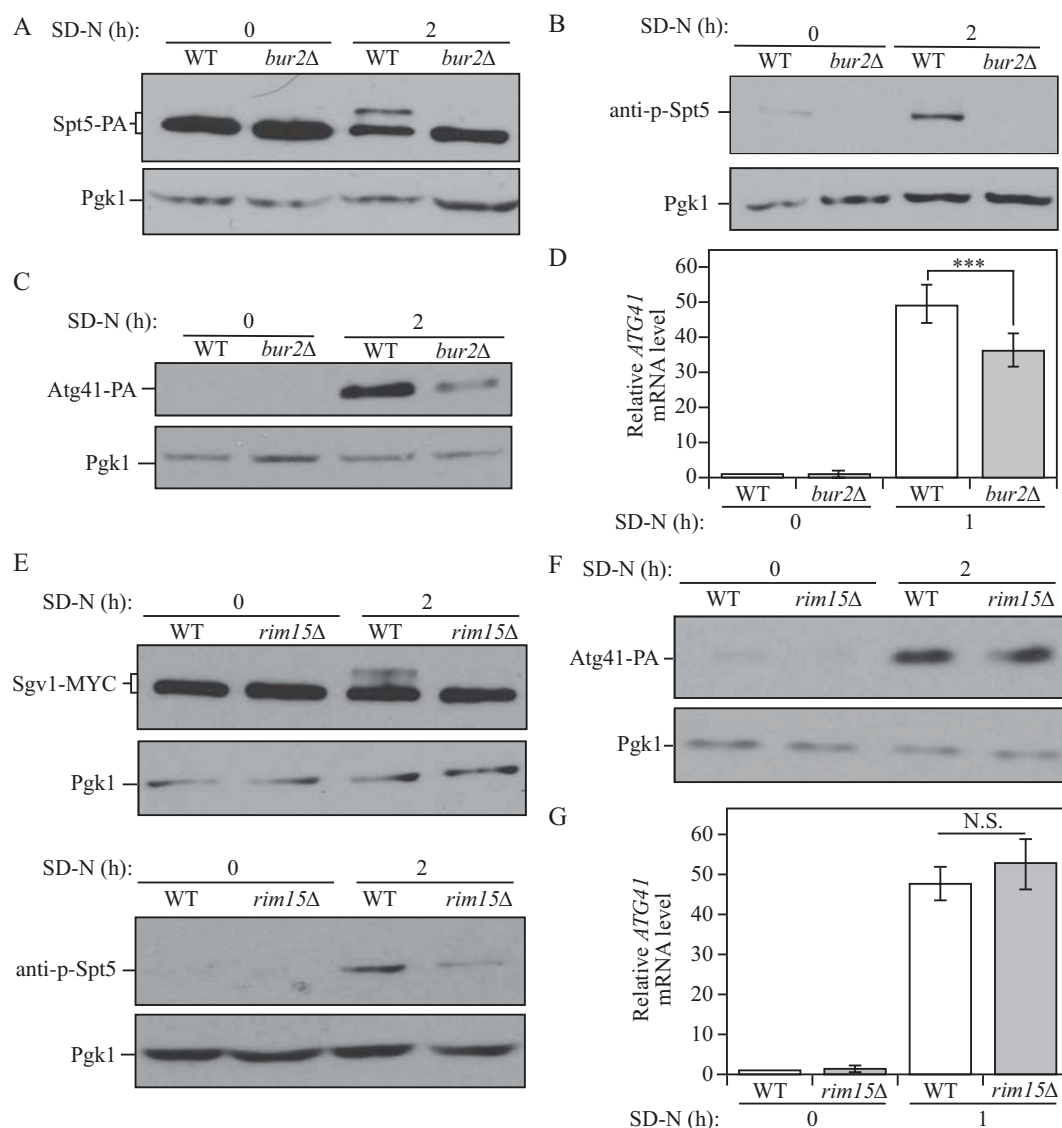


Figure 5. The Sgv1-Bur2 complex is responsible for Spt5 phosphorylation after starvation, and Sgv1 is phosphorylated under starvation conditions by the Rim15 kinase. **(A)** Samples from the Spt5-PA wild-type (WXY102) and *bur2Δ* (WXY104) strains were collected in both growing (YPD) and starvation (SD-N) conditions for western blot analysis. Anti-PA antibody and anti-Pgk1 antiserum were used to detect the indicated proteins. **(B)** The Spt5 phosphorylation was detected with anti-p-Spt5 antibody in wild-type (WLY176) and *bur2Δ* (WXY115) samples collected from growing (YPD) and starvation (SD-N, t = 2 h) conditions. **(C)** The Atg41-PA level was probed with anti-PA antibody in wild-type (ZYY108) and *bur2Δ* (WXY116) cells from growing (YPD) and starvation (SD-N, t = 2 h) conditions. **(D)** The wild-type (WLY176) and *bur2Δ* (WXY115) cells were cultured until mid-log phase in growing conditions (YPD) and then shifted to starvation conditions (SD-N) for 1 h. The mRNA level of *ATG41* was measured by RT-qPCR. The error bar represents the SEM of 3 independent experiments, and p values are reported for the comparison between the wild-type and *bur2Δ* strains during starvation. ***, p < 0.005. **(E)** The Sgv1-MYC wild-type (WXY117) and *rim15Δ* (WXY120) strains were grown in YPD to mid-log phase and then shifted to starvation conditions (SD-N) for 2 h. The samples were then collected and analyzed by western blot using antibodies to MYC. The samples from wild-type (WLY176) and *rim15Δ* (WXY123) cells were also collected and Spt5 phosphorylation was detected with the anti-p-Spt5 antibody. Pgk1 was used as the loading control. **(F)** The Atg41-PA wild-type (ZYY108) and *rim15Δ* (WXY124) cells were collected in both growing (YPD) and starvation (SD-N) conditions for western blot analysis. Anti-PA antibody and anti-Pgk1 antiserum were used to detect the indicated proteins. **(G)** RT-qPCR analysis of *ATG41* mRNA level in WT (WLY176) and *rim15Δ* (WXY123) cells under growing and starvation conditions. The error bar represents the SEM of 3 independent experiments.

We extended this analysis by examining an additional Spt5 mutant. In this case, we transformed centromeric plasmids expressing *SPT5* WT and mutant (MUT; which contains an Spt5 derivative with 15 potentially phosphorylated C-terminal domain serine residues changed to alanine) into the Spt5-inducible degradation strain. These strains thus contain 2 copies of *SPT5* after transformation; the application of auxin resulted in the degradation of the WT Spt5-AID-MYC. After starvation, WT cells treated with

the chemical carrier DMSO and probed with the anti-p-Spt5 phospho-specific antiserum displayed 2 bands (Figure S4A). The upper band corresponded to the phosphorylated Spt5 from the WT chromosomally integrated Spt5-AID-MYC, whereas the lower band marked the position of phosphorylated Spt5 expressed from the plasmid; only the WT form of the latter protein, not the [S15A] version, was detected with the anti-p-Spt5 serum. After auxin treatment, Spt5-AID-MYC was completely degraded

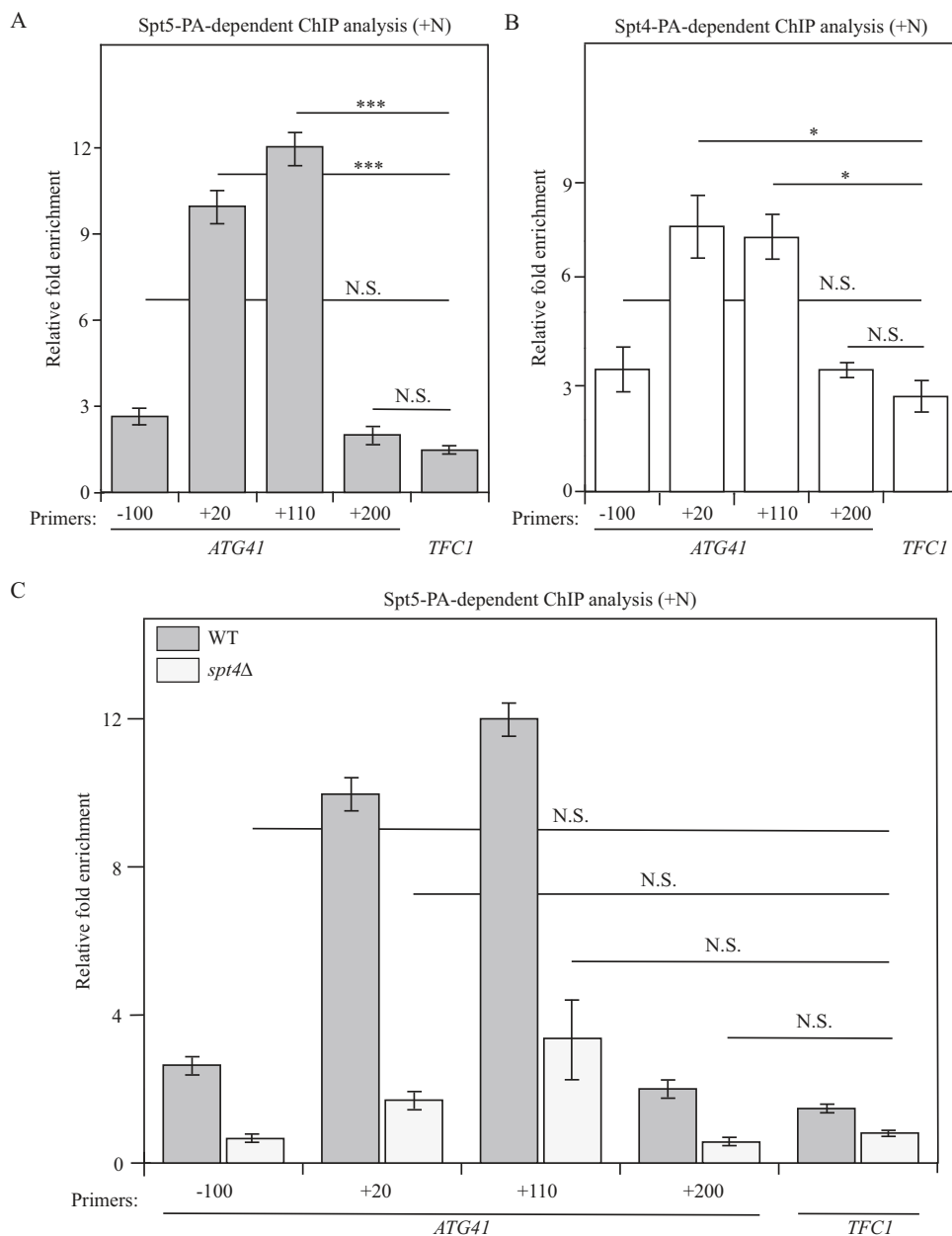


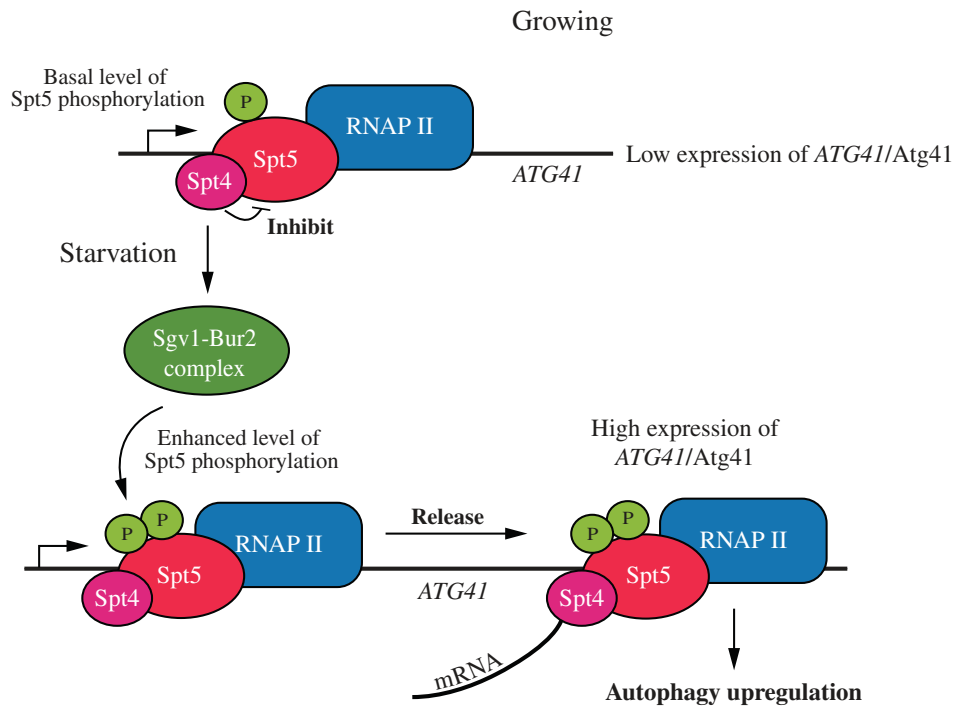
Figure 6. Spt5 binds to *ATG41* DNA in an Spt4-dependent manner. **(A-C)** Chromatin immunoprecipitation (ChIP) was done in Spt5-PA (WXY102), Spt4-PA (WXY106) and *spt4Δ* Spt5-PA (WXY103) strains. The ChIP samples were collected in the growing condition (mid-log phase). RT-qPCR was used for quantitative analysis. The primers for ChIP cover different DNA regions from the promoters through the ORF in *ATG41*. “-” indicates upstream of the *ATG* start codon, and “+” indicates downstream of the *ATG* start codon. **(A)** RT-qPCR analysis of ChIP samples of the Spt5-PA (WXY102) strain. The values were normalized to the input. The error bars show the SEM of at least 3 independent experiments. p values in each region are reported for the comparison with the negative control, *TFC1*. ***, $p < 0.005$; N.S., not significant. **(B)** RT-qPCR analysis of ChIP samples of the Spt4-PA (WXY106) strain. The error bars show the SEM of at least 3 independent experiments: *, $p < 0.05$; N.S., not significant. **(C)** RT-qPCR analysis of ChIP samples of Spt5-PA (WXY102) and *spt4Δ* Spt5-PA (WXY103) cells. The values were normalized to the input DNA. *TFC1* was used as a negative control and the error bars represent the SEM of at least 3 independent experiments. The significance analysis for *spt4Δ* strains was noted: N.S., not significant.

so that the only species of Spt5 that remained was derived from the plasmid. In the nutrient-depleted condition, we observed a decreased *ATG41* mRNA level in mutant cells with auxin treatment whereas the *ATG8* mRNA level showed no change (Figure S4B); this was similar to results from Spt5[S7A] cells (Figure 4D and Figure S2A). Therefore, we conclude that Spt4 plays a negative role in regulating *ATG41* in growing conditions, and that this inhibitory role is reversed by Spt5 phosphorylation when autophagy is induced.

The Sgv1/Bur1-Bur2 complex phosphorylates Spt5 after starvation

Yeast Sgv1/Bur1, which is similar in sequence to mammalian P-TEFb, can phosphorylate the C-terminal domain of both Spt5 and RNAP II under normal growth conditions [27]. Sgv1 forms a complex with the regulatory protein Bur2, a divergent cyclin; the Sgv1-Bur2 complex together plays a role in regulating transcription [31]. Although *SGV1* is essential, *BUR2* is not an essential gene. Therefore, we analyzed Spt5-PA phosphorylation

A Wild-type cells



B

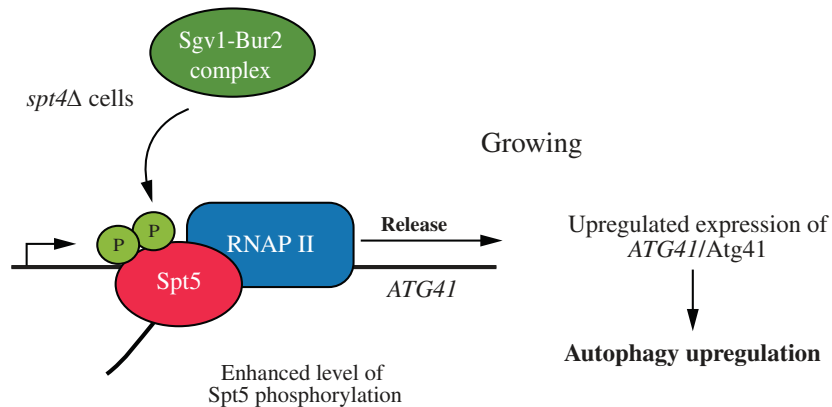


Figure 7. A model for Spt4-Spt5-dependent regulation of *ATG41*. **(A)** In wild-type cells under growing conditions, the Spt4-Spt5 complex may inhibit transcription of *ATG41* through an Spt4-dependent interference with Spt5 phosphorylation, causing the complex to accumulate near the TSS. After starvation, phosphorylation of Spt5 by the Sgv1-Bur2 kinase complex releases the inhibitory effect of Spt4 on *ATG41* transcription, and the Spt4-Spt5 complex participates in transcription elongation. **(B)** In *spt4Δ* cells, Spt5 does not accumulate near the TSS of *ATG41*, and transcription actively proceeds. Spt5 can also be more efficiently phosphorylated upon the deletion of *SPT4*.

in WT and *bur2Δ* cells. The band shift of Spt5 that was observed in the WT strain following autophagy induction disappeared in *bur2Δ* mutant cells (Figure 5A). The phosphorylated band was also absent in the mutant cells probed with the anti-p-Spt5 antibody (Figure 5B). Therefore, the Sgv1-Bur2 complex is responsible for the observed phosphorylation of Spt5 in starvation conditions. Because the deletion of *BUR2* was sufficient to block the phosphorylation of Spt5, we further used the *bur2Δ* strain to examine its influence on *ATG41*. In the nutrient-deficient condition, both mRNA and protein levels of *ATG41/Atg41* decreased when *BUR2* was deleted (Figure 5C,D), which corresponded to our observations with the nonphosphorylatable Spt5[S7A] mutant (Figure 4D,E).

In addition, we extended our analysis on the regulation of Spt5 by examining potential connections with other kinases in regulating autophagy. Rim15 plays a crucial role in integrating many nutrient-regulatory signals, and previous work from our lab has found that Rim15 positively regulates autophagy activity [32]. In *rim15Δ* cells, phosphorylation of the Sgv1 kinase was suppressed, and the phosphorylation of Spt5 was largely, but not completely, blocked under starvation conditions (Figure 5E), suggesting that Rim15 may function upstream of the Sgv1-Bur2 complex to control Spt5. However, mRNA and protein levels of *ATG41/Atg41* showed no clear difference in the *rim15Δ* mutant, indicating that the partial block of Spt5 phosphorylation was not enough to affect *ATG41* expression (Figure 5F,G). Atg1

is the only protein kinase in the core autophagy machinery [33], and we further tested its potential effect on Spt5 phosphorylation. In *atg1Δ* cells, we could detect a partial decrease of the Spt5 phosphorylated band after starvation, but there was no significant change in *ATG41* mRNA level (Figure S5A,B), which was similar to the phenotype of *rim15Δ* cells (Figure 5F,G). These results suggest that, after starvation, a small population of phosphorylated Spt5 may be sufficient to induce *ATG41* expression.

Spt5 binds to *ATG41* DNA in an Spt4-dependent manner

Based on the above experiments, the Spt4-Spt5 complex plays a major role in regulating *ATG41*/Atg41 expression. Thus, we decided to investigate the mechanism through which the Spt4-Spt5 complex regulates the transcription of *ATG41*. Because this complex is a transcription factor, we used a chromatin immunoprecipitation (ChIP) approach in both Spt5-PA and Spt4-PA strains to test whether this complex can directly bind to DNA. We designed several pairs of primers, each spanning approximately 130 to 170 nucleotides of different regions from the promoter to the open reading frame (ORF) of *ATG41*. The results showed that the +20 base pair (bp) and +110 bp regions in the ORF of *ATG41* were highly enriched in the DNA fragments precipitated with Spt5-PA, suggesting that Spt5 might bind tightly to these regions when autophagy is not induced (Figure 6A). A similar enrichment was also observed in the Spt4-PA strain in growing conditions (Figure 6B). The relative accumulation of the Spt4-Spt5 complex at these 2 regions near the TSS presumably reflects the normal situation, and thus maintains low expression of *ATG41* in growing conditions. In contrast, we did not observe an enrichment of *ATG1* DNA bound to Spt5-PA and Spt4-PA (Figure S6A,B), in agreement with the lack of an effect of Spt4 on *ATG1* expression (Figure 1E and Figure S1D). In *spt4Δ* cells, the mRNA level of *ATG41* increased dramatically (Figure 1E), indicating active transcription of *ATG41* when Spt4 was absent. Accordingly, the increase in the enrichment of the *ATG41* +20 bp and +110 bp regions with Spt5-PA ChIP went down in *spt4Δ* cells compared to WT cells, suggesting a release from the temporary “halting” at the early stage of *ATG41* transcription (Figure 6C). Taken together, we propose that in nutrient-rich conditions, Spt4 acts negatively on Spt5, interfering with phosphorylation of the latter, and causing the complex to accumulate at regions near the *ATG41* TSS; this regulation is part of the mechanism that functions to maintain a low, basal level of gene expression.

Discussion

When facing different environmental stress conditions, it is important to finely tune the magnitude of autophagy in order to maintain cell homeostasis and prevent diseases. The efficient response of autophagy requires the upregulation of many *ATG* genes, among which *ATG8* and *ATG41* display the most dramatic changes. Previous studies from our lab have identified 2 transcription factors in autophagy: Ume6 as a repressor of *ATG8*, and Gcn4 as an activator of *ATG41* [11,13]. We found that the absence of Ume6 did not affect the level of Atg41 (Figure S7A). However, our understanding

about the transcriptional regulation of even these genes is still limited. Here, we present data supporting a previously unknown negative role of Spt4 in regulating the expression of *ATG8* and *ATG41* in budding yeast. Furthermore, Spt4 is the first identified negative transcriptional regulator of *ATG41*, and this negative function was not due to a change of Gcn4 expression (Figure S7B).

The heterodimeric Spt4-Spt5 complex is a highly conserved transcription regulator, and it can tightly bind to the coiled domain of RNAP II in a transcription-dependent manner [34]. Many studies have revealed the essential role of the Spt4-Spt5 complex in promoting transcription elongation, and, in more complex eukaryotes, further work on DSIF (the Spt4-Spt5 homolog), in conjunction with the NELF complex, has indicated the existence of a mechanism that pauses transcription at the early stage. Genome-wide studies have revealed that pausing is widespread in mammalian cells, defined by a temporary halt of transcription within ~100 nucleotides downstream of the TSS [35]. The release from pausing relies on phosphorylation of the SUPT5H C terminus by the P-TEFb kinase, thereby changing the status of DSIF to positively regulate transcription elongation [18]. Follow-up precision run-on sequencing (PRO-seq) studies have also identified a promoter-proximal pause-like phenomenon in fission yeast [20].

However, in other organisms that lack NELF such as *S. cerevisiae*, currently there are no reports showing a role of the Spt4-Spt5 complex in transcriptional pausing; although PRO-Seq data provide an indication that Spt4 may have some negative role in transcription [20]. Compared to the published large-scale genome studies, our data show that the Spt4-Spt5 complex may act in a gene-specific manner in budding yeast, with Spt4 having an additional and clear negative role for certain *ATG* genes under growing conditions. This type of regulation fits with the observation that stress-response genes, such as *ATG* genes are regulated in a manner that is opposite to most genes encoding proteins that function during vegetative growth [36,37]. The deletion of *SPT4* leads to an increase of *ATG8*/Atg8 and *ATG41*/Atg41, and the change in *ATG41* expression in particular facilitates an increase in autophagy activity. After starvation, we observed an enhanced phosphorylation of Spt5. Of note, Spt5 phosphorylation also increases when *SPT4* is absent. Accordingly, the dephosphorylation of Spt5 results in a clear autophagy deficiency and a significant decrease in *ATG41* expression, which demonstrates that Spt5 phosphorylation is important for regulating autophagy after starvation, with Spt4 having a largely negative role in regulation for *ATG41*. The deletion of *BUR2*, the regulatory partner of the Sgv1 kinase complex, blocks Spt5 phosphorylation and leads to a lower expression of *ATG41*/Atg41, further suggesting the importance of Spt5 phosphorylation in *ATG41* transcription. In addition, both Spt4 and Spt5 can bind to the DNA region in the ORF of *ATG41*, whereas the absence of Spt4 prevents the accumulation of Spt5 at the *ATG41* TSS, suggesting that Spt4 might influence the function of Spt5 by controlling its access to the Sgv1 kinase, and its subsequent interaction with DNA (Figure 7).

There are still many remaining questions that await further analysis. For example, although Spt4 plays a negative role in regulating *ATG8/Atg8* expression, and both Spt4 and Spt5 can bind to specific regions on *ATG8* DNA (Figure S8A,B), Spt5 phosphorylation seems not to be the reason for *ATG8* upregulation after starvation, because dephosphorylation of Spt5 causes no significant changes in the level of *ATG8*. However, the deletion of *BUR2* leads to a decreased level of *ATG8/Atg8* (Figure S8C,D). Therefore, there appears to be another unknown mechanism behind the Sgv1-Bur2 kinase complex to directly regulate *ATG8*. Moreover, compared to the very large increase (~10 fold) of the *ATG41* mRNA level seen in *spt4Δ* cells, *ATG8* exhibits a rather milder increase of ~2 fold. However, the ratio of upregulated protein level of Atg8 is similar to that of Atg41 in the *spt4Δ* mutant in vegetative conditions. Similarly, in the *ume6Δ* strain, the *ATG8* mRNA level increases ~3 fold (Figure S8E), while the protein level shows a substantially more dramatic change [13]. This leads us to propose that there are other downstream factors that influence the protein level of Atg8 after transcription. Another question that remains to be answered is how the Sgv1 kinase complex senses the starvation signal and further enhances the phosphorylation of Spt5. Rim15 seems to be a good candidate for phosphorylating Sgv1 when autophagy is induced, but its direct effect on *ATG41* is not clear. Finally, our initial exploration of the negative function of Spt4 with regard to particular *ATG* genes was based on a raw large-scale PRO-seq analysis (data not shown), but it will also be important to determine what other genes that may affect autophagy, if any, are negatively regulated by Spt4.

Here, for the first time we have revealed a negative role of Spt4 within the Spt4-Spt5 complex in regulating transcription in budding yeast. Furthermore, Spt4 and Spt5 carry out different functions with regard to the regulation, in which Spt4 has a negative function in growing conditions whereas Spt5 is always required for efficient transcription. Because autophagy plays a crucial physiological role, and its dysfunction is associated with many diseases, our results can also advance an understanding of the transcriptional control of autophagy, which may provide new directions for future therapeutics.

Materials and methods

Yeast strains, media and culture conditions

Yeast strains used are listed in Table S1. We applied standard methods to generate gene deletions and/or for C-terminal tagging [38,39]. Yeast cells were grown in rich medium at 30°C (YPD: 1% [w:v] yeast extract, 2% [w:v] peptone, and 2% [w:v] glucose). Autophagy was induced upon nitrogen starvation by shifting mid-log phase cells from YPD to SD-N (0.17% yeast nitrogen base without ammonium sulfate or amino acids, and 2% [w:v] glucose) for the indicated times.

Antibodies and antisera

Anti-YFP antibody, which detects GFP, was from Clontech (JL-8; 63281), anti-PA antibody was from Jackson Immuno Research (323-005-024), anti-MYC was from Sigma (M4439),

and anti-Pgk1 is a generous gift from Dr. Jeremy Thorner (University of California, Berkeley). Anti-p-Spt5 antibody was generously provided by Dr. Steven Hahn [27]. Antibodies to Ape1, Atg1 and Atg8 were described previously [40–42].

Plasmids

GFP-Atg8(405) contains the GFP-Atg8 open reading frame with the endogenous *ATG8* promoter. pCu-GFP-ATG8(405) was constructed by replacing the endogenous *ATG8* promoter with the *CUP1* promoter, containing the GFP-Atg8 open reading frame [43]. These plasmids were linearized and integrated into the corresponding strains listed in Table S1. Plasmids expressing Flag-tagged WT Spt5 and Spt5[S15A] were provided by Dr. Steven Hahn [27].

Real-time quantitative PCR

Yeast cells were cultured in YPD to mid-log phase and shifted to SD-N for autophagy induction. Total RNA was extracted with an RNA extraction kit (NucleoSpin RNA II; Clontech, 740955.50), and reverse transcription was undertaken using the High Capacity cDNA Reverse Transcription Kit (ThermoFisher Scientific, 4368814). RT-qPCR was performed using the Power SYBR Green PCR Mix (ThermoFisher Scientific, 4367659) or Radiant Green Lo-ROX qPCR kit (Alkali Scientific, QS1020). All primer information can be found in Table S2.

Auxin-inducible degron (AID) system and transcriptional inhibition

WLY176 cells were first transformed with the plasmid pNHK53 (*ADH1p-OsTIR1-9MYC*; National BioResource Project–Yeast [Japan]), and Spt5 was then tagged with AID-9MYC (Addgene, 99522; deposited by Dr. Helle Ulrich) by homologous recombination. The auxin-inducible degron (AID) refers to the 71–116 amino acids of the AT1G04250/ATIAA17 protein in plants. To control Spt5 protein levels, the cells were treated with 300 μM 3-indoleacetic acid (auxin; Sigma, I2886) or DMSO (vehicle) in the vegetative condition for 30 min to induce degradation of Spt5. Then the cells were shifted to SD-N for nitrogen starvation with application of auxin or DMSO. After 1 h of starvation and treatment, samples were collected for western blot and RNA extraction.

Chromatin immunoprecipitation (ChIP)

ChIP was performed with some modifications from a method described previously [44]. The strains that are used in the study are Spt5-PA (WXY102), Spt4-PA (WLY106) and *spt4Δ* Spt5-PA (WXY103). After yeast cells grew to OD₆₀₀ ~ 0.8 in YPD medium, a final concentration of 1% formaldehyde was added to perform cross-linking and the cultures were shaken for 20 min at room temperature. Glycine was added to 0.2 M to stop cross-linking. Samples were then harvested, washed in PBS and resuspended in FA lysis buffer (50 mM HEPES, pH 7.5, 150 mM NaCl, 1 mM EDTA, 1% Triton X-100 [Sigma, T8787], 0.1% sodium deoxycholate [Sigma, D6750], 0.1%

SDS). The cells were lysed with glass beads by being vortexed at 4°C, and then were centrifuged at 1000 x g for 1 min. The supernatant was collected for sonication (4 cycles of 25 s on, 59 s off, pulse at a power output of 20%) at 4°C. Sonicated samples were collected by centrifugation, and the supernatant was collected and then divided into input and IP fractions. Half of the IP fractions were incubated with IgG Sepharose 6 Fast Flow beads (Fisher Scientific, 45-000-173) while the other half were incubated with PA beads (“non-antibody” mock control) for 4 h at 4°C. After immunoprecipitation, the beads were washed with FA lysis buffer and wash buffer (10 mM Tris-HCl, pH 8.0, 0.25 M LiCl, 1 mM EDTA, 0.5% Nonidet P-40 [IGEPAL; Fisher Scientific, NC9983875], 0.5% sodium deoxycholate), resuspended in elution buffer (50 mM Tris-HCl, pH 7.5, 10 mM EDTA, 1% SDS) and incubated at 70°C for 12 min (with mixing by vortex every 3 min). With the addition of proteinase K (Fisher Scientific, NC9404543), reverse cross-linking was performed by incubation for 2 h at 42°C followed by 6 h at 65°C. The reverse cross-linked samples were then incubated with RNase A (Qiagen, 19,101) at 37°C for 30 min. The purified DNA was examined by RT-qPCR analysis, which was performed using the Power SYBR Green PCR Mix (ThermoFisher Scientific, 4367659). The information for all primers is listed in Table S2.

Other methods

Western blot, GFP-Atg8 processing, and prApe1 processing were described previously [3].

Statistical analysis

Two-tailed Student’s t test and two-tailed paired Student’s t test were used to determine statistical significance.

Acknowledgments

The authors thank Drs. Vivian Cheung and Isabel Wang for helpful comments and technical advice, and Dr. Steven Hahn for providing reagents.

Disclosure statement

No potential conflict of interest was reported by the authors.

Funding

This work was supported by the National Institute of General Medical Sciences [GM131919] (DJK); and by the Swiss National Science Foundation [31003A-166482/1] (JD).

ORCID

Daniel J. Klionsky  <http://orcid.org/0000-0002-7828-8118>

References

- [1] Yang Z, Klionsky DJ. Eaten alive: a history of macroautophagy. *Nat Cell Biol.* 2010;12(9):814–822.
- [2] Klionsky DJ, Cregg JM, Dunn WA, et al. A unified nomenclature for yeast autophagy-related genes. *Dev Cell.* 2003;5(4):539–545.
- [3] Klionsky DJ, Abdelmohsen K, Abe A, et al. Guidelines for the use and interpretation of assays for monitoring autophagy (3rd edition). *Autophagy.* 2016;12(1):1–222.
- [4] Feng Y, He D, Yao Z, et al. The machinery of macroautophagy. *Cell Res.* 2014;24(1):24–41.
- [5] Baba M, Takeshige K, Baba N, et al. Ultrastructural analysis of the autophagic process in yeast: detection of autophagosomes and their characterization. *J Cell Biol.* 1994;124(6):903–913.
- [6] Yang Z, Klionsky DJ. An overview of the molecular mechanism of autophagy. *Curr Top Microbiol Immunol.* 2009;335:1–32.
- [7] He C, Klionsky DJ. Regulation mechanisms and signaling pathways of autophagy. *Annu Rev Genet.* 2009;43:67–93.
- [8] Wen X, Klionsky DJ. An overview of macroautophagy in yeast. *J Mol Biol.* 2016;428(9 Pt A):1681–1699.
- [9] Reggiori F, Klionsky DJ. Autophagic processes in yeast: mechanism, machinery and regulation. *Genetics.* 2013;194(2):341–361.
- [10] Shintani T, Klionsky DJ. Autophagy in health and disease: a double-edged sword. *Science.* 2004;306(5698):990–995.
- [11] Yao Z, Delorme-Axford E, Backues SK, et al. Atg41/Icy2 regulates autophagosome formation. *Autophagy.* 2015;11(12):2288–2299.
- [12] Xie Z, Nair U, Klionsky DJ. Atg8 controls phagophore expansion during autophagosome formation. *Mol Biol Cell.* 2008;19(8):3290–3298.
- [13] Bartholomew CR, Suzuki T, Du Z, et al. Ume6 transcription factor is part of a signaling cascade that regulates autophagy. *Proc Natl Acad Sci U S A.* 2012;109(28):11206–11210.
- [14] Hartzog GA, Fu J. The Spt4-Spt5 complex: a multi-faceted regulator of transcription elongation. *Biochim Biophys Acta.* 2013;1829(1):105–115.
- [15] Wada T, Takagi T, Yamaguchi Y, et al. DSIF, a novel transcription elongation factor that regulates RNA polymerase II processivity, is composed of human Spt4 and Spt5 homologs. *Genes Dev.* 1998;12(3):343–356.
- [16] Yamaguchi Y, Takagi T, Wada T, et al. NELF, a multisubunit complex containing RD, cooperates with DSIF to repress RNA polymerase II elongation. *Cell.* 1999;97(1):41–51.
- [17] Yamada T, Yamaguchi Y, Inukai N, et al. P-TEFb-mediated phosphorylation of hSpt5 C-terminal repeats is critical for processive transcription elongation. *Mol Cell.* 2006;21(2):227–237.
- [18] Ni Z, Saunders A, Fuda NJ, et al. P-TEFb is critical for the maturation of RNA polymerase II into productive elongation in vivo. *Mol Cell Biol.* 2008;28(3):1161–1170.
- [19] Chen Y, Yamaguchi Y, Tsugen Y, et al. DSIF, the Paf1 complex, and Tat-SF1 have nonredundant, cooperative roles in RNA polymerase II elongation. *Genes Dev.* 2009;23(23):2765–2777.
- [20] Booth GT, Wang IX, Cheung VG, et al. Divergence of a conserved elongation factor and transcription regulation in budding and fission yeast. *Genome Res.* 2016;26(6):799–811.
- [21] Ammerer G, Hunter CP, Rothman JH, et al. PEP4 gene of *Saccharomyces cerevisiae* encodes proteinase A, a vacuolar enzyme required for processing of vacuolar precursors. *Mol Cell Biol.* 1986;6(7):2490–2499.
- [22] Rondon AG, García-Rubio M, González-Barrera S, et al. Molecular evidence for a positive role of Spt4 in transcription elongation. *Embo J.* 2003;22(3):612–620.
- [23] Klionsky DJ, Emr SD. Membrane protein sorting: biosynthesis, transport and processing of yeast vacuolar alkaline phosphatase. *Embo J.* 1989;8(8):2241–2250.
- [24] Klionsky DJ. Monitoring autophagy in yeast: the Pho8Delta60 assay. *Methods Mol Biol.* 2007;390:363–371.
- [25] Shintani T, Klionsky DJ. Cargo proteins facilitate the formation of transport vesicles in the cytoplasm to vacuole targeting pathway. *J Biol Chem.* 2004;279(29):29889–29894.
- [26] Scott SV, Nice III DC, Nau JJ, et al. Apg13p and Vac8p are part of a complex of phosphoproteins that are required for cytoplasm to vacuole targeting. *J Biol Chem.* 2000;275(33):25840–25849.

- [27] Liu Y, Warfield L, Zhang C, et al. Phosphorylation of the transcription elongation factor Spt5 by yeast Bur1 kinase stimulates recruitment of the PAF complex. *Mol Cell Biol.* 2009;29(17):4852–4863.
- [28] Swaney DL, Beltrao P, Starita L, et al. Global analysis of phosphorylation and ubiquitylation cross-talk in protein degradation. *Nat Methods.* 2013;10(7):676–682.
- [29] Holt LJ, Tuch BB, Villén J, et al. Global analysis of Cdk1 substrate phosphorylation sites provides insights into evolution. *Science.* 2009;325(5948):1682–1686.
- [30] Morawska M, Ulrich HD. An expanded tool kit for the auxin-inducible degron system in budding yeast. *Yeast.* 2013;30(9):341–351.
- [31] Wood A, Shilatifard A. Bur1/Bur2 and the Ctk complex in yeast: the split personality of mammalian P-TEFb. *Cell Cycle.* 2006;5(10):1066–1068.
- [32] Yorimitsu T, Zaman S, Broach JR, et al. Protein kinase A and Sch9 cooperatively regulate induction of autophagy in *Saccharomyces cerevisiae*. *Mol Biol Cell.* 2007;18(10):4180–4189.
- [33] Kamada Y, Funakoshi T, Shintani T, et al. Tor-mediated induction of autophagy via an Apg1 protein kinase complex. *J Cell Biol.* 2000;150(6):1507–1513.
- [34] Tardiff DF, Abruuzzi KC, Rosbash M. Protein characterization of *Saccharomyces cerevisiae* RNA polymerase II after in vivo cross-linking. *Proc Natl Acad Sci U S A.* 2007;104(50):19948–19953.
- [35] Scheidegger A, Nechaev S. RNA polymerase II pausing as a context-dependent reader of the genome. *Biochem Cell Biol.* 2016;94(1):82–92.
- [36] Hu G, McQuiston T, Bernard A, et al. The role of transcriptional ‘futile cycles’ in autophagy and microbial pathogenesis. *Microb Cell.* 2015;2(8):302–304.
- [37] Gatica D, Hu G, Liu X, et al. The Pat1-Lsm complex stabilizes ATG mRNA during nitrogen starvation-induced autophagy. *Mol Cell.* 2019;73(2):314–324 e4.
- [38] Longtine MS, McKenzie A, Demarini DJ, et al. Additional modules for versatile and economical PCR-based gene deletion and modification in *Saccharomyces cerevisiae*. *Yeast.* 1998;14(10):953–961.
- [39] Gueldener U, Heinisch J, Koehler GJ, et al. A second set of loxP marker cassettes for Cre-mediated multiple gene knockouts in budding yeast. *Nucleic Acids Res.* 2002;30(6):e23.
- [40] Klionsky DJ, Cueva R, Yaver DS. Aminopeptidase I of *Saccharomyces cerevisiae* is localized to the vacuole independent of the secretory pathway. *J Cell Biol.* 1992;119(2):287–299.
- [41] Abeliovich H, Zhang C, Dunn WA, et al. Chemical genetic analysis of Apg1 reveals a non-kinase role in the induction of autophagy. *Mol Biol Cell.* 2003;14(2):477–490.
- [42] Huang WP, Scott SV, Kim J, et al. The itinerary of a vesicle component, Aut7p/Cvt5p, terminates in the yeast vacuole via the autophagy/Cvt pathways. *J Biol Chem.* 2000;275(8):5845–5851.
- [43] Geng J, Nair U, Yasumura-Yorimitsu K, et al. Post-Golgi Sec proteins are required for autophagy in *Saccharomyces cerevisiae*. *Mol Biol Cell.* 2010;21(13):2257–2269.
- [44] Aparicio O, Geisberg JV, Sekinger E, et al. Chromatin immunoprecipitation for determining the association of proteins with specific genomic sequences in vivo. *Curr Protoc Mol Biol.* 2005; Chapter 21:Unit 21 3.